A road bridge dynamic response analysis by wavelet and other estimation techniques

A ROAD BRIDGE DYNAMIC RESPONSE ANALYSIS BY WAVELET AND OTHER ESTIMATION TECHNIQUES

A. Fasana, L. Garibaldi, E. Giorcelli, S. Marchesiello, M. Ruzzene

Dipartimento di Meccanica
Politecnico di Torino
C.so Duca degli Abruzzi, 24
10129 Torino
ITALY
fasana@polito.it - garibaldi@polito.it - ruzzene@polito.it

ABSTRACT - In this paper, a dynamic test performed over a bridge located in northern Italy is reported: the dynamic measures are analysed by means of three different techniques to seek for the best algorithm within those appropriate for the identification of dynamic systems excited by unknown input.
The bridge under test, in fact, is excited by the flowing traffic and by some other unmeasured excitations as wind or other ground micro-movements; the analysis based on the flowing traffic excitation has shown to be extremely advantageous for the road contractors, i.e. in the case of motorway, because it can be adopted for monitoring in-use roads, without the need of traffic stop. The accelerometers data have been used for the identification of the natural frequencies, viscous damping ratios and mode shapes of the bridge. The modal parameters have been extracted using three approaches (ARMAV, CVA et WET) and a comparison within the performances of the adopted methods is also given.
A FEM model has been set-up by using 8 nodes brick elements based only on a rough sketch of the bridge: this was used to optimise the position of the reference accelerometers.
Due to the limited number of points measured along the bridge, the extracted experimental shapes have been expanded into a larger number of points to accomplish a minimum set of locations coincident with the FEM nodes; this expansion has been performed by means of the Guyan expansion based on the numerical modes. The non-symmetric distribution of the updated stiffness matrix ΔK has shown the differences with the original model and a few comments are reported as possible explanations of the bridge real behaviour.

***RESUME** - Dans cet article, on présente les tests dynamiques sur un pont autoroutier dans le nord de l'Italie: les mesures ont été analysées en utilisant trois techniques différentes parmi celles développées pour l'identification des systèmes dynamiques avec des excitations inconnues.*
Le pont considéré est sollicité soit par le trafique soit par le vent et micro mouvements du terrain; ce genre de analyse dynamique est très convénients pour les compagnies gérantes les autoroutes, puisqu'il permet de contrôler le comportement du pont dans les conditions d'usage habituelles, sans besoin de arrêter le trafique. Les accélérations mesurées ont été utilisées pour l'identification des fréquences naturelles, des amortissements et des modes du pont. Ces paramètres ont été estimés avec trois techniques (ARMAV, CVA et WET) et une comparaison entre ces méthodes est présentée dans l'article.
Un modèle simplifié aux éléments finis a été réalisé en utilisant des éléments 'brick' à 8 nodes et a été utilisé pour étudier la dispositions optimale des accéléromètres.
Vu le numéro limité des points de mesure, les modes expérimentaux ont dû être étendus, en utilisant la technique SEREP, pour obtenir un numéro suffisant de positions coincidantes avec les nodes du modèle. La distribution non symétrique de la matrice ΔK recalée a montré des différences avec le modèle original, et quelques explications sur le comportement réel du pont sont présentées.

1. INTRODUCTION

The dynamic of bridges has been extensively studied in recent years due to the increasing interest in the monitoring techniques to predict and the lifetime of the structure or, more realistically, to assess the best maintenance program.
Many conferences around the world, as well as many journals concerning the dynamics of large structures have extensively treated this matter [IMAC, SPIE, etc].
Up to now, the dynamic monitoring is still in a development phase, being the current techniques sometimes difficult to apply, too expensive or simply not sufficiently sensitive.
The paper presents a review of a few methods currently used and highlights the pro and cons of the different procedures. At the end, an attempt of system updating is also given through five different methods: this is done nevertheless the quality of the measurements and the modal parameters extracted is suffering from the poor number of the acquisition points.

2. BRIDGE DESCRIPTION

The bridge we deal with in this paper is a simply supported structure 20 meters long and approximately 10 meters wide. The acceleration responses have been measured in 7 points along one edge of the bridge and in 2 points along the other, for a total of 9 measured points. A sketch of the accelerometers disposition and of the measured structure is presented in Figure 1, where the black dots indicate the reference locations. More details on the experimental set-up, together with some results can be found in [1] and [2].

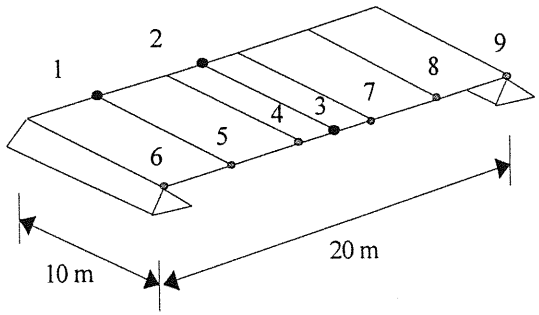

Figure 1: Sketch of the bridge and measured points location.

3. THE WAVELET ESTIMATION TECHNIQUE (WET)

The Wavelet Transform (WT) of the signal $x(t)$ is defined as follows:

$$W_g(a,b) = \frac{1}{\sqrt{a}} \cdot \int_{-\infty}^{+\infty} x(t) \cdot g^*\left(\frac{t-b}{a}\right) dt \tag{1}$$

where $g^*(t)$ is the complex conjugate of the analysing wavelet $g(t)$, dilated by the scale parameter a and translated along the time axis by parameter b. The WT performs a linear decomposition of the analysed signal in the time-scale domain, the time decomposition being given by b and the scale domain decomposition being given by a.
There are several functions that can be used as analysing wavelets and in this work Morlet's Wavelet:

$$g(t) = e^{j \cdot \omega_w \cdot t} \cdot e^{-\frac{t^2}{2}} \tag{2}$$

has been considered , being ω_w the wavelet's frequency.
The scale decomposition of the signal can be related to a frequency domain decomposition by considering the dilated version of the Fourier Transform of $g(t)$:

$$G(a \cdot \omega) = \sqrt{2 \cdot \pi} \cdot e^{-\frac{1}{2}(a \cdot \omega - \omega_w)^2} \tag{3}$$

The value of frequency where the analysing wavelet is focused is the one giving a maximum value to $G(a \cdot \omega)$, that is $a \cdot \omega = \omega_w$.
The resolution of the wavelet decomposition in the time-frequency domain is determined by the duration Δt_g and bandwidth Δf_g of the analysing wavelet and by the value of the dilation parameter a [3,4]:

$$\Delta t = a \Delta t_g; \qquad \Delta f = \Delta f_g / a \tag{4}$$

The resolution of the analysis therefore results good for high dilation in the frequency domain and for low dilation in the time domain.

3.1 Natural frequencies and modal damping ratios

A very interesting property of the WT, discussed in detail in [3], consists in its capability of demodulating the analysed signal both in amplitude and phase. If a general kind of signal is considered:

$$x(t) = k(t) \cdot \cos(\varphi(t) \cdot t) \tag{5}$$

where $k(t)$ and $\varphi(t)$ are time-varying envelope and phase functions, the WT of $x(t)$ has the following expression:

$$W(a,b) = \sqrt{a} \cdot k(b) \cdot e^{-(a \cdot \varphi(b) - \omega_w)^2} \cdot e^{j \cdot \varphi(b) \cdot b} \tag{6}$$

for a fixed value of the dilation parameter a ($a=a_i$), that is for a fixed frequency:

$$\begin{aligned} |W(a_i,b)| &= \sqrt{a_i} \cdot k(b) \cdot e^{-(a_i \cdot \varphi(b) - \omega_w)^2} \\ \angle[W(a_i,b)] &= \varphi(b) \cdot b \end{aligned} \tag{7}$$

being $|W(a_i,b)|$ and $\angle[W(a_i,b)]$ the modulus and the phase of the WT.

Equation (7) shows how general time varying envelope $k(t)$ and phase $\varphi(t)$ can be effectively determined using the modulus and the phase of the WT, for a fixed value of frequency.
The wavelet representation in the time-frequency domain results also very useful when the analysed signal is the free response of a MDOF system. The time-frequency maps allow to follow the decay of each mode of the structure separately from the others, only by selecting the right frequency value corresponding to the mode of interest. Using this wavelet property, it is possible to follow the envelope decay and the phase variation in the time domain of each modal component and to estimate the corresponding damping ratio and natural frequency.

3.2 Mode shapes estimation

When the transient time responses recorded from several points of the structure are available, phase and amplitude relationships between the different degrees of freedom of the system can be easily detected through the WT analysis. The j-th mode shape of the structure can be estimated by evaluating the WT of the time signals from all the measured points, at the corresponding j-th frequency. Let for example be $Wh_k(b,a_j)$ and $Wh_r(b,a_j)$ the WTs of the signals at point k and at the reference point r respectively. It is easy to notice how their ratio:

$$\frac{Wh_k(b,a_j)}{Wh_r(b,a_j)} = \psi_{kj} \tag{8}$$

is, in a noise-free case, constant with respect to time b. The quantity $\psi_{kj} = r_{kj} + i*s_{kj}$ represents the k-th component of the j-th complex mode shape of the structure, including amplitude and phase information, referred to the reference point. When real data are considered, some errors may occur because of the presence of noise and equation (8) will estimate a component $\tilde{\psi}_{kj} = \tilde{r}_{kj} + i*\tilde{s}_{kj} \neq \psi_{kj}$. It can be shown that the values of $\tilde{r}_{kj}, \tilde{s}_{kj}$ giving the best estimate of the mode shape component, that is minimising the following error function:

$$e_k = \sum_{i=1}^{n} \left| Wh_k(b_i,a_j) - \tilde{\psi}_{kj} \cdot Wh_r(b_i,a_j) \right|^2 \tag{9}$$

are:

$$r_{kj} = \frac{\sum_{i=1}^{n} q_k(b_i,a_j)\cdot q_r(b_i,a_j)}{\sum_{i=1}^{n} q^2{}_r(b_i,a_j)}; \quad s_{kj} = \frac{\sum_{i=1}^{n} q_k(b_i,a_j)\cdot p_r(b_i,a_j)}{\sum_{i=1}^{n} q^2{}_r(b_i,a_j)} \tag{10}$$

being $q_k(b_i,a_j)=Re[Wh_k(b_i,a_j)]$, $p_k(b_i,a_j)=Im[Wh_k(b_i,a_j)]$ and n the number of time samples.

4. THE ARMAV TECHNIQUE

A general overview of the ARMAV technique can be found in many recent papers by the present authors [5-8] and by other research groups. This technique has already been applied in many circumstances, for bridge, dams, or building monitoring. In many of the these cases, the excitation is due to the flowing wind or ground micromovements, which are far to represent white noise, but are still better than the traffic excitation. For this case, in fact, a procedure to verify the proper characteristics of the signals is needed.
Considering the stationarity of the signal is rarely respected over a relatively long acquisition period (i.e. for the typical record lengths used in bridge testing), shorter data time spans can be adopted for the ARMAV analysis, being the method well suited and properly working over very short data (i.e. hundred data points).
The ARMAV model has the following structure, described by a matrix difference equation:

$$\bar{x}[n] = \sum_{k=1}^{p} A[k]\bar{x}[n-k] + \bar{u}[n] + \sum_{k=1}^{q} B[k]\bar{u}[n-k] \tag{11}$$

where $\bar{x}[n]$; $\bar{u}[n] \in \mathbf{R}^g$ and $A[k]$; $B[k] \in \mathbf{R}^{g,g}$
Its poles are defined by the following matrix equation:

$$det\left(I - \sum_{k=1}^{p} A[k]\, z^{-k} \right) = 0 \quad \Rightarrow \quad p_k \ , \quad k = 1,..,g\cdot p \tag{12}$$

which is a higher order eigenvalue problem with $g\cdot p$ solutions. The ARMAV model can be expressed in the state space to obtain the following expression:

$$\left\{\underline{x[n]}\right\} = [a]\left\{\underline{x[n-1]}\right\} + [b]\left\{\underline{u[n]}\right\} \tag{13}$$

This expression can be used to estimate the model parameters $\left(A[k]\right)_{i,j}$ and the algorithm can be organised in order to split the main problem into g sub problems to be solved by an iterative method.

Once the model parameters have been estimated it's possible to solve equation (12) to find out the poles p_k ; to reach this result it's necessary to compute the eigenvalues of the following auxiliary matrix:

$$A = \begin{bmatrix} 0 & I & \cdots & & \\ \vdots & \vdots & \cdots & \vdots & 0 \\ & 0 & \cdots & I & \\ & & \cdots & & I \\ A[1] & A[2] & \cdots & A[p-1] & A[p] \end{bmatrix} \tag{14}$$

Its eigenvectors express also the "modal vectors" of the ARMAV model.

In these parametric models the system output $\bar{x}[n]$ is supposed to be caused by a white noise input $\bar{u}[n]$ and the algorithm estimates the parameters' values that minimise the residual variance.

4.1 ARMAV parameter estimation

It's possible to demonstrate that the discrete ARMAV(n, n-1) model is equivalent to a linear continuous system of order n. Since we are analysing second order systems, ARMAV(2,1) models are adopted.

The parameter estimation algorithm works as follows: a first ARV model, whose structure is:

$$\bar{x}[n] = \sum_{k=1}^{p} \hat{A}[k]\,\bar{x}[n-k] + \hat{\bar{u}}[n] \tag{15}$$

is fitted to the data; consequently, using the estimated autoregressive parameters $\hat{A}[k]$, the residual vector $\hat{\bar{u}}[n]$ is estimated.

These estimated residual time series are used as input $\hat{\bar{u}}[n]$ in the ARMAV model:

$$\bar{x}[n] = \sum_{k=1}^{p} \hat{A}[k]\,\bar{x}[n-k] + \hat{\bar{u}}[n] + \sum_{k=1}^{q} \hat{B}[k]\,\hat{\bar{u}}[n-k] \tag{16}$$

and so an iterative procedure can be started, to alternately refine the estimated parameters $\hat{A}[k]$, $\hat{B}[k]$ and the residual $\hat{\bar{u}}[n]$ to minimise the residual variance.

The procedure ends when the difference between the parameters $\hat{A}[k]$ and $\hat{B}[k]$, estimated in two consecutive iterations, is smaller than a desired value.

4.2 Data verification

Some enhancements in the ARMAV technique can be obtained by adopting a pre-screening of the data, i.e. by checking the statistical characteristics of the raw time histories and their properties. This procedure, which has already been presented in [2], is based on the idea that the closer the Probability Density Function (PDF), calculated on the data, to the theoretical Gaussian distribution, the better the final quality of the results of the ARMAV technique [9]. In previous papers [5-8], the Gaussianity was usually underestimated, being the method sufficiently robust to determine the modal characteristics anyway, while in this case we found out that this control can be very effective to forecast the correct convergence of the routine.

In Figure 2, the PDF obtained by the signal corresponding to the accelerometers located in position 2, in Figure 1, (one fourth of the span) and 4 (near the support) are reported; it is evident how the PDF is close to gaussianity for location 4 only, corresponding to an almost fixed point. All the other locations with a non-negligible mobility show the same statistical behaviour as location 2.

For this reason, a parameter giving the distance of the accelerometer data with respect to the Gaussian curve was hence computed in order to check the quality of the available data. In particular, this parameter has been used in order to choose the best data blocks suitable for the analysis.

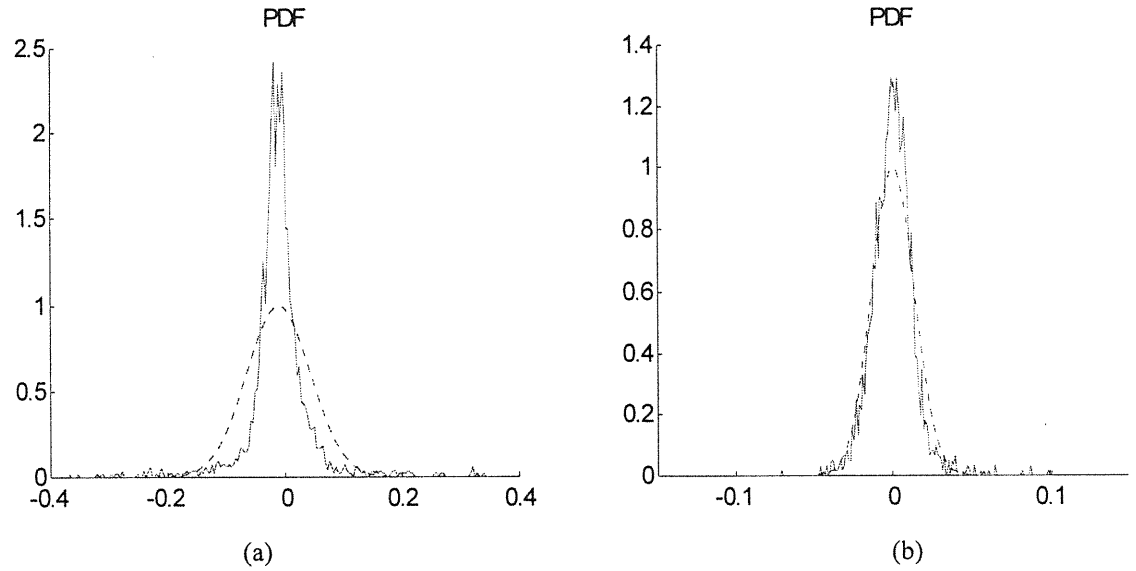

Figure 2. Time histories and their PDF for location 2 (a) and location 4 (b), near the support (see Figure 1).

5. THE CANONICAL VARIATE ANALYSIS (CVA)

In order to compare the results of the ARMAV and WET methods, another technique has been here investigated, which is based on the following stochastic state space system:

$$\begin{aligned} x(k+1) &= Ax(k) + w(k) \\ y(k) &= Cx(k) + v(k) \end{aligned} \tag{17}$$

where $w(k)$ is the process noise and $v(k)$ is the measurement noise, both assumed to be zero mean, white vector sequences; moreover, $x(k)$ and $y(k)$ are the state vector of dimension n and the output vector of dimension N_{resp} respectively at discrete time instant k. The eigenvalue decomposition of the discrete state matrix A is:

$$A = \Psi \Lambda \Psi^{-1} \tag{18}$$

with Λ the diagonal matrix of discrete eigenvalues (λ_1 ,..., λ_n). These can be transformed into continuous eigenvalues (μ_i) of the mechanical system as follows:

$$\mu_i = \frac{1}{\Delta t} ln(\lambda_i) \tag{19}$$

The mode shapes at the sensor locations are the columns of Φ, given by:

$$\Phi = C\Psi \,. \tag{20}$$

Let now the (block) Hankel matrix $H_{p,p}$ and the covariance (block) matrices $\Re^+$ and $\Re^-$ be [10]:

$$H_{p,p} = \begin{bmatrix} \Gamma(1) & \Gamma(2) & . & . & \Gamma(p) \\ \Gamma(2) & \Gamma(3) & . & . & \Gamma(p+1) \\ . & . & . & . & . \\ \Gamma(p) & \Gamma(p+1) & . & . & \Gamma(2p-1) \end{bmatrix} \tag{21}$$

$$\Re^+ = \begin{bmatrix} \Gamma(0) & \Gamma'(1) & . & . & \Gamma'(p-1) \\ \Gamma(1) & \Gamma(0) & . & . & \Gamma'(p-2) \\ . & . & . & . & . \\ \Gamma(p-1) & \Gamma(p-2) & . & . & \Gamma(0) \end{bmatrix} \tag{22}$$

$$\Re^{-} = \begin{bmatrix} \Gamma(0) & \Gamma(1) & . & . & \Gamma(p-1) \\ \Gamma'(1) & \Gamma(0) & . & . & \Gamma(p-2) \\ . & . & . & . & . \\ \Gamma'(p-1) & \Gamma'(p-2) & . & . & \Gamma(0) \end{bmatrix} \tag{23}$$

where p is a user defined parameter and Γ_k are the sampled covariance matrices, given by:

$$\Gamma_k = \frac{1}{M}\sum_{m=0}^{M} y(m+k)y'(m) \tag{24}$$

M being the number of observations and ' denoting transposition. These empirical covariance matrices substitute the expected values $\Gamma_k = E[y(m+k)y'(m)]$ defined in [10], giving empirical Hankel and Toeplitz matrices. Let the full-rank factorisation of $\Re^{+}$ and $\Re^{-}$ be:

$$\Re^{+} = L^{+}(L^{+})', \ \Re^{-} = L^{-}(L^{-})' \tag{25}$$

The normalised Hankel matrix has the following singular-value decomposition:

$$\overline{H}_{p,p} = (L^{+})^{-1} H_{p,p}((L^{-})')^{-1} = \begin{bmatrix}[U_1] & [U_2]\end{bmatrix}\begin{bmatrix}[S_1] & [0] \\ [0] & [S_2]\end{bmatrix}\begin{bmatrix}[V_1]' \\ [V_2]'\end{bmatrix} \tag{26}$$

with: $[S_1]=\text{diag}(\sigma_1,\ldots,\sigma_n)$, $\sigma_1 \geq \sigma_2 \ldots \sigma_n \geq 0$

$$[S_2]=\text{diag}(\sigma_{n+1},\ldots,\sigma_{pNresp}),\ \sigma_{n+1} \geq \sigma_{n+2} \ldots \sigma_{pNresp} \geq 0 \tag{27}$$

The model order n is generally selected so that $\sigma_n >> \sigma_{n+1}$, but often stabilisation diagrams are more suitable to find the correct model order. The last step of the procedure consists in defining the extended observability and controllability matrices as follows:

$$O_p = \begin{bmatrix} C \\ CA \\ . \\ CA^{p-1} \end{bmatrix}; C_p = \begin{bmatrix} G & AG & \ldots & A^{p-1}G \end{bmatrix} \tag{28}$$

where $G=E[x(k+1)y'(k)]$. Then the model parameters will be estimated from:

$$A = (S_1)^{-0.5} U_1'(L^{+})^{-1} H^{\uparrow}_{p,p}((L^{-})')^{-1} V_1 (S_1)^{-0.5}$$

$$C=\text{first } p \text{ rows of } O_p = L^{+}U_1(S_1)^{0.5} \tag{29}$$

where $H^{\uparrow}_{p,p}$ is the $H_{p,p}$ shifted up by p rows.

In order to select the physical modes stabilisation diagrams for both eigenfrequencies and damping ratios are then needed. Furthermore the stabilisation between two consecutive mode shapes is evaluated by performing the Modal Assurance Criterion, given by:

$$MAC(i,j) = \frac{\left|\Phi_i^{H}\Phi_j\right|^2}{\left(\Phi_i^{H}\Phi_i\right)\left(\Phi_j^{H}\Phi_j\right)} \tag{30}$$

where H is the complex transposed.

Another, slightly different, stochastic subspace identification method, called Balanced Realisation in [11], simply requires the Singular Value Decomposition of the matrix $H_{p,p}$, that is equivalent to setting $L^{+}=I$ and $L^{-}=I$ in (26) and (29), so no weighting for the Hankel matrix is involved.

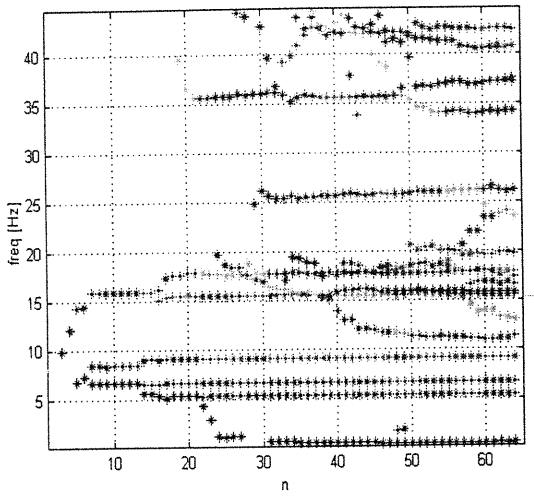

Figure 3: Global Frequency Stabilisation Diagram

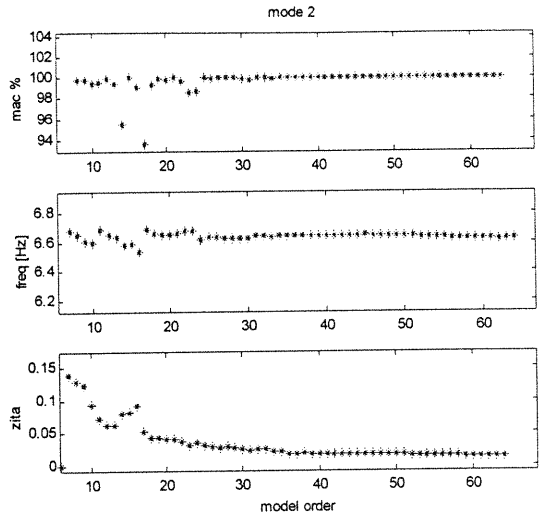

Figure 4: Stabilisation diagrams for mode n° 2: MAC, frequency and damping

6. COMPARISON OF RESULTS

The three methods presented above have been applied to analyse the acceleration data measured on the bridge and to extract its modal parameters. The estimated natural frequencies are presented in Table 1, where the results from the three methods are compared (WET, ARMAV and CVA) and also the results obtained from a slightly different stochastic identification method, mentioned in section 5, called here MBH, simply requiring the Singular Value Decomposition of the matrix $H_{p,p}$ in equation (29) are included.

Table 1: Natural frequencies and estimations standard deviations

	WET		ARMAV		MBH		CVA	
Mode	Frequency [Hz]	σ_f [Hz]	Frequency [Hz]	σ_f [Hz]	Frequency [Hz]	σ_f [Hz]	Frequency [Hz]	σ_f [Hz]
1	5.25	0.00	5.27	0.11	5.33	0.10	5.29	0.16
2	6.36	0.13	6.68	0.10	6.61	0.06	6.59	0.17
3	8.99	0.03	8.97	0.13	8.83	0.15	9.03	0.27
4	15.21	0.32	15.61	*	15.51	0.11	15.65	0.17
5	17.86	0.25	17.61	*	17.79	0.12	17.78	0.20

*Not enough samples

A very good agreement can be found between all the methods in the natural frequencies estimations, even if for modes 2 and 4 the frequencies estimated by the WET result slightly lower than the others. We should here mention the fact that these techniques belong to completely different philosophies: the ARMAV and the Stochastic Subspace techniques, coming both from the Control Systems area, give a black-box approach to the identification problem, since they analyse all the time data simultaneously, while the WET performs the analysis on each time history.

Table 2: Damping ratios and estimations standard deviations

	WET		ARMAV		MBH		CVA	
Mode	ζ [%]	σ_ζ [%]	ζ [%]	σ_ζ [%]	ζ [%]	σ_ζ [%]	ζ [%]	σ_ζ [%]
1	0.2	0.08	3.0	0.93	2.4	0.78	4.5	0.75
2	1.0	0.32	1.8	0.91	2.4	0.89	3.7	1.32
3	1.6	0.38	1.4	0.37	1.8	0.61	2.3	0.84
4	1.4	0.94	3.0	*	1.5	0.36	2.6	1.14
5	0.8	0.16	2.6	*	0.8	0.21	1.7	0.49

*Not enough samples

The identification of the damping ratios (Table 2) results, as usual, very crucial. In particular, the results concerning the first mode are in great disagreement, the WET giving a value of the damping ratio much smaller than the ones estimated by the other methods. We should however consider that the first mode resulted much less excited than the second and the third, for instance, the signal to noise ratio associated to it being therefore very low.
In estimations of the damping associated to the other modes (2 to 5) some encouraging similarities can be however found. The uncertainties in damping estimations, do not allow us to choose the method assuring the best accuracy on damping.

7. THE UP-DATING TECHNIQUES

An attempt has been done to apply a few different up-dating procedures on the parameter extracted with the methods seen in previous paragraphs.
First of all, it should be mentioned that the number of measured points over the structure is too low to allow a reliable estimation of the modified stiffness of the structure. For this reason, the measured points have been expanded into a larger number by using a Guyan expansion which takes advantage of the numerical shapes obtained by a FEM model of the original structure. The new matrix composed by 27 points and five modes has been used to up-date the model by means of five procedures: i.e. the methods by Sidhu-Ewins, Chen, Dobson, Gaukrogen, Berman-Baruch.
While the first two methods faced some numerical problems due to the ill-conditioning of the system, the other three have obtained almost the same positive results, as confirmed by the MAC values between the measured and the updated modes (Table 3).
As already mentioned, the ΔK matrix determined by all these methods is mainly reconstructed from the numerical model, hence giving larger errors for the real measured points and negligible discrepancies for those co-ordinates generated by the Guyan expansion. Only one of these matrices is reported in Figure 5, being the others very similar.
It can be seen how the stiffness modifications mainly affect the corner closer to the view, i.e. the original nine measured co-ordinates.

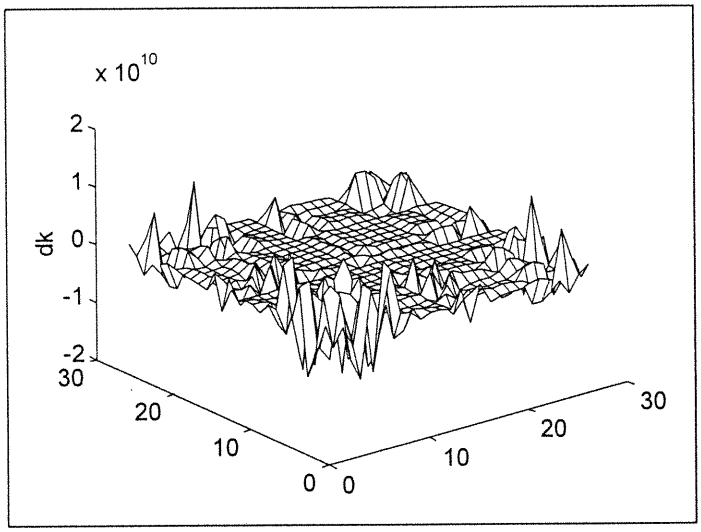

Figure 5: ΔK matrix for Dobson's up-dating procedure

Table 3: MAC between FEM and experimental modes

1.000	0.078	0.150	0.078	0.003
0.078	1.000	0.030	0.129	0.000
0.150	0.030	1.000	0.000	0.000
0.078	0.129	0.000	1.000	0.001
0.003	0.000	0.000	0.001	1.000

Due to the poor data, no deductions can be made on the presence of possibly damaged areas, being the map too affected by the expansion procedure.
On the other side, an analytical fitting of the modes can be advantageously employed as already done by many authors: in this specific case, however, the lack of some fundamental co-ordinates, as those on the midline of the bridge, leads to a misinterpretations of the modes, hence giving origin to an ill-conditioned problem.

8. CONCLUSIONS

The only-output measurement techniques, as ARMAV and CVA-MBH, have already demonstrated their robustness and reliability when applied to stochastically excited MDOF's systems. Particularly, dealing with the problem of real bridges under traffic load, it has been demonstrated the advantage to carry on the identification procedure without requiring the traffic slow-down or interruption. On the occasion of these tests, we have sought for the robustness of these methods, even for those cases where data are particularly non-stationary and non-Gaussian.
It should be reminded, however, that the bridge test here presented suffered for the low number of measurement points, hence giving a very poor spatial resolution in computing the mode shapes, not presented in the paper as being those of a simply supported plate.
Particularly, the poor spatial resolution strongly affects the application of up-dating techniques, as can be deduced from most of the literature on this topic. This is probably the challenge of the future work in bridge damage identification, which has recently reached very enhanced results in terms of data fitting and system identification procedures, but still suffers for the low spatial resolution when employed for damage identification and localisation.

9. REFERENCES

1. Piombo B., Fasana A., Marchesiello S., Ruzzene M., "Modelisation and identification of the dynamic response of a supported bridge" NATO-ASI Modal Analysis and Testing, Sesimbra, Portugal, May 3-15, pp. 523-534, 1998.
2. Garibaldi L., Giorcelli E., Marchesiello S., "ARMAV Technique enhancements for traffic excited bridge" NATO-ASI Modal Analysis and Testing, Sesimbra, Portugal, May 3-15 pp. 717-724, 1998.
3. Ruzzene M., Fasana A., Garibaldi L., Piombo B., "Natural frequencies and dampings identification using Wavelet Transform: application to real data" Mechanical Systems and Signal Processing **11**(2), 207-218, 1997.
4. Chui C.K., *Wavelets analysis and applications: an introduction to wavelets.* Vol. 1, Academic Press Inc., 1992
5. Piombo B., Garibaldi L., Giorcelli E., Fasana A., "Structures Identification using ARMAV models", Proceedings XI IMAC, Kissimmee (Florida), USA, February 1993.
6. Riva A., Garibaldi L., Giorcelli E., Fasana A., "Modal analysis and system identification using ARMAV models", XII IMAC, Honolulu (Hawaii), USA, 31 January- 3 February 1994.
7. Giorcelli E., Riva A., Garibaldi L., Fasana A., "ARMAV analysis of Queensborough bridge ambient data", XIV IMAC, Dearborn (Michigan), USA, 12 -15 February 1996.
8. Giorcelli E., Garibaldi L., Piombo B., "ARMAV techniques for traffic excited bridges", accepted for pubblication, ASME Journal of Vibration and Acoustics, July 1998.
9. Sabia L., "Identificazione strutturale in regime lineare e non-lineare", PhD Thesis, Politecnico di Torino, 1998.
10. Desai U.B., Debajyoti P., Kirkpatrick R.D., "A realisation approach to stochastic model reduction", Int. J. of Control, Vol. 42(4), pp. 821-838, 1985.
11. Hermans L., Van der Auweraer H., "Modal testing and analysis of structures under operational conditions: industrial applications", NATO-ASI Modal Analysis and Testing, Sesimbra, Portugal, May 3-15, pp. 549-563, 1998.
12. Fasana A., Garibaldi L., Piombo B., Ruzzene M., "Identification of the dynamic behaviour of bridges under ambient excitation Using Wavelet Transform" Proceedings Non Destructive Evaluation (NDE) SPIE Conference, Scottsdale, Arizona, 3-5 december 1996.
13. Fasana A., Garibaldi L., Piombo B., Ruzzene M., "Application of the Wavelet Estimation Technique for the analysis of a motorway bridge." Proceedings of the DAMAS Conference, Sheffield, U.K., June 30- July 2 1997.
14. Fasana A., Garibaldi L., Giorcelli E., Ruzzene M., Sabia D., "Analysis of a motorway bridge under random excitation", XV IMAC, Orlando (Florida), USA, 3 - 6 February 1997.
15. Kirkegaard P. H., Andersen P. "State space identification of civil engineering structures from output only measurements", XV IMAC, Orlando (Florida), USA, 3 - 6 February 1997.